

## Electrospun carbon nanofibers (CNFs) modified with needle-like SiC nanostructures

Weronika Pazdyk-Słaby, Elżbieta Długoń, Dariusz Zientara,  
Aneta Fraczek-Szczypta\*

AGH University of Krakow, Faculty of Materials Science and Ceramics,  
al. Mickiewicza 30, 30-059 Kraków

\*Corresponding author, e-mail: [afraczek@agh.edu.pl](mailto:afraczek@agh.edu.pl)

ORCID numbers

Weronika Pazdyk-Słaby: 0000-0001-6751-7061

Elżbieta Długoń: 0000-0003-4698-7595

Dariusz Zientara: 0000-0002-6931-3043

Aneta Fraczek-Szczypta: 0000-0002-2055-1489

### Abstract

Electrospun carbon nanofibers (CNFs) are an excellent material which can possess a wide range of properties through controlling the parameters of the electrospinning process, as well as through thermal treatment. At the same time, CNFs are an excellent substrate for carrying out modifications, both volumetric, at the stage of precursor preparation, and surface modifications. Different methods of introducing various silicon carbide (SiC) precursors into the spinning solution enables the formation of needle-shaped SiC nanostructures on the CNF surface.

This work presents an attempt to obtain nanofibrous carbon materials modified in volume and on the surface with SiC precursors, along with their characteristics. The most promising method of creating needle-like SiC nanostructures on the surface of CNFs is the use of volume modification with polysiloxane and silanization of the surface of the CNFs in a organosilicon sol solution.

This article has been accepted for publication and undergone full peer review but has not been through the copyediting, typesetting, pagination and proofreading process which may lead to differences between this version and the version of record. Please cite this article as DOI: [10.24425/cpe.2024.149469](https://doi.org/10.24425/cpe.2024.149469).

Received: 23 April 2024 | Revised: 25 June 2024 | Accepted: 04 September 2024



**Keywords:** electrospinning, carbon nanofibers, ceramics, composite materials, silicon carbide

## 1. Introduction

Carbon nanomaterials, such as carbon nanotubes or carbon nanofibers, have been receiving considerable interest in the field of environmental protection, especially in water purification processes. The special properties of electrospun carbon nanofibers (CNFs) mean that these materials have already been used as a reinforcement for nanocomposites, in biomedical engineering, as catalyst carriers, sensors, and galvanic cells (Soltani et al., 2022). CNFs are characterised by high mechanical strength, low density, additionally they are chemically stable and conduct electricity well (Sharon, 2021). The potential of CNFs obtained by electrospinning lies in the possibility of carrying out various modifications and optimisations at various stages of their preparation allowing to produce a material with the desired morphology, structure and functionality (Tan et al., 2024). The prospect of producing carbon-ceramic hybrid materials can make it possible to produce nanocomposites with improved structural, microstructural and physicochemical properties. Thanks to the unique combination of the properties of CNFs with resistance to high temperatures, oxidation, and high chemical stability of ceramic materials such as silicon carbide (SiC), the obtained hybrid materials can operate in difficult conditions (Koyanagi et al., 2021). Carbon-ceramic nanocomposites seem to be an interesting material for use in membrane technologies for water treatment (Cheng et al., 2018). Membrane technologies face the problem of biofouling, caused by the multiplication of micro- and macro-organisms causing the formation of a biofilm on the membrane surface. In our previous work, we reported a modification of electrospun carbon nanofibers with metal nanoparticles with antibacterial properties (Pazdyk-Slaby et al., 2024). Due to the difficult operating conditions of membranes in filtration processes, new technological solutions are being sought. The development of carbon-ceramic composites seems to be justified in this case. The introduction of a ceramic phase improves chemical stability and increases resistance to oxidation and high temperatures. Moreover, there are reports in the literature indicating the antibacterial influence of SiC nanofibrous structures through toxic effects on the bacterial cells, increasing the efficiency of the membrane (Szala and Borkowski, 2014).

There are known examples of the use of electrospun PAN fibers in environmental protection. NaOH-activated hydrothermal carbon-coated PAN fibers show potential for herbicide removal from agricultural wastewater (Zhao et al., 2016). Efficient TEOS-modified carbon nanofiber membranes have been developed for the filtration of metal

nanoparticles and their oxides (Au, Ag, TiO<sub>2</sub>) from aqueous solutions (Faccini et al., 2015). It has been proven that coating carbon nanofibers with SiC/SiO<sub>2</sub> improves oxidation resistance and thermal degradation of materials significantly decreases (Kim et al., 2010). A SiC coating was produced on the CNF surface using a mixture of Si and SiO<sub>2</sub> powders in an argon atmosphere. The SiC coating inhibits the formation of CNF agglomerates, and the resulting composite is characterized by increased cracking resistance compared to monolithic SiC (Xu et al., 2014).

In the present work, an attempt was made to produce and characterise CNFs modified with needle-like SiC nanostructures. So far, there has been no information in the literature about hybrid CNF systems - needle-like SiC nanostructures, which would be obtained as a result of heat treatment of PAN nanofibers modified with polysiloxane, TEOS and organosilicon sol. These SiC precursors are not as popular as SiO<sub>2</sub> described in the literature (Dai et al., 2017), and their use for the modification of CNF is the added value of this publication.

## 2. Experimental

### 2.1. Formation and thermal treatment of PAN nanofibers and silanization

Two types of modification of carbon nanofibers with SiC precursors were carried out: volumetric and surface. For this purpose, three precursor solutions of 10% polyacrylonitrile (PAN, Sigma Aldrich) dissolved in N,N-dimethylformamide (DMF, Avantor) were prepared. PAN used to prepare spinning solutions was dried for 24 h at temperature of 75 °C and pressure of 0.2 bar. Then, two types of SiC precursors were added to two of them – tetraethoxysilane (TEOS, Sigma Aldrich) and polysiloxane (Lukosil M 130) in weight to PAN ratios of 1:1. PAN polymer nanofibers were obtained using the electrospinning method. Under the influence of high voltage, polymer nanofibers were formed from the spinning solutions and collected on a rotating collector. The parameters for obtaining nanofibers were as following: nozzle diameter 1.1 mm; collector-nozzle distance 60 mm, voltage 10 kV, formation time 90 min, and the collector rotation speed 4 RPM. The environmental parameters were as follows: temperature 25 °C, humidity ~ 30–35 %. The obtained PAN nanofibers were converted into carbon nanofibers as a result of thermal treatment including stabilization, carbonization and high-temperature treatment. Stabilization was carried out in an air atmosphere, in two stages at 240 °C and 260 °C. Carbonization consisted of heating the samples in a nitrogen atmosphere from RT to 800 °C, with a heating rate of 5 °C/min. After reaching this temperature, the samples were kept there for 60 minutes

and then cooled to RT. The last stage of processing was heating the samples at a rate of 10 °C/min in N<sub>2</sub> to a temperature of 1550 °C and holding them for 60 minutes.

The obtained samples were marked as follows:

CNF – electrospun carbon nanofibers,

CNF/polysiloxane – volumetrically modified carbon nanofibers with polysiloxane,

CNF/TEOS – volumetrically modified carbon nanofibers with TEOS.

Surface modification was already carried out on CNF as a result of the silanization process in sol. The synthesized sol contained T and D structural units in molar proportions  $\frac{T}{D} = \frac{4}{1}$ . The T unit is present in methyltrimethoxysilane, the silicon atom is connected to one alkyl group and three alkoxy groups. The D unit occurs in dimethyldiethoxysilane, where the silicon atom is connected to two alkyl and two alkoxy groups. To prepare the sol, monomers of methyltriethoxysilane and dimethyldiethoxysilane were used, anhydrous ethyl alcohol as a solvent, dilute hydrochloric acid as a catalyst and distilled water to initiate the hydrolysis reaction. The sample was immersed in the sol solution for 2 days. After this time, it was dried in air at 70 °C for 7 days. The dried sample was heat treated at 800 °C and at 1550 °C under the conditions previously described.

The received material was marked:

CNF/sol – carbon nanofibres silanized in sol  $\frac{T}{D} = \frac{4}{1}$ .

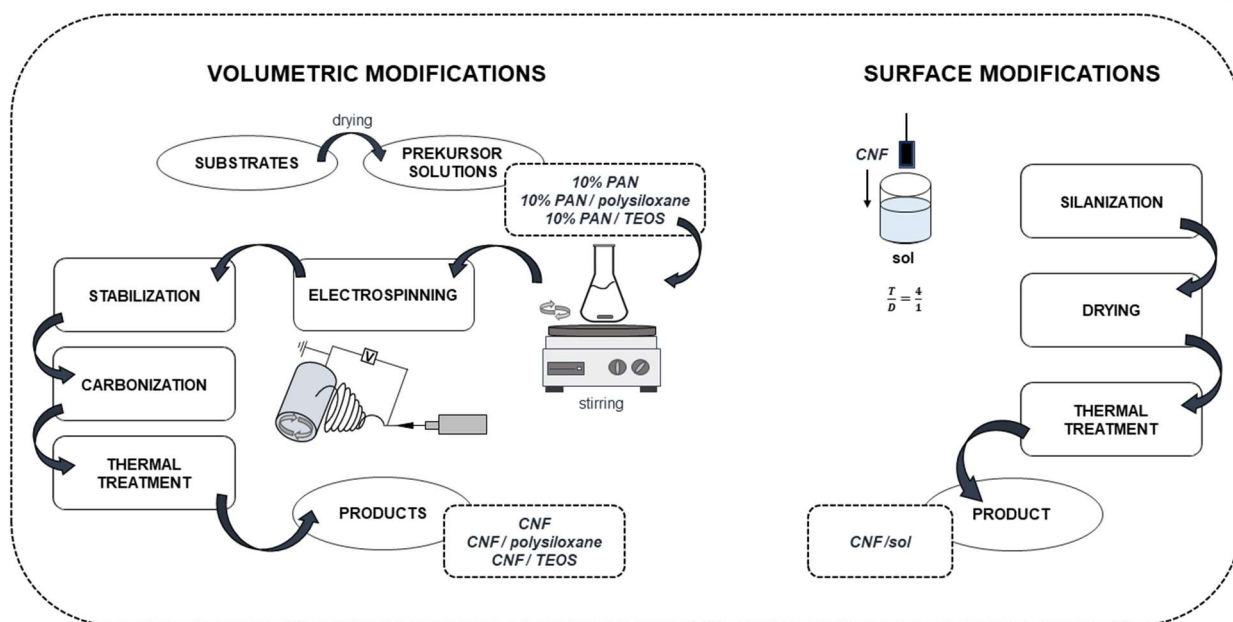


Figure 1. Schematic illustration of the preparation process of CNF - needle-like SiC nanostructures.

## 2.2. Characterization

Using Nova NanoSEM 200 (FEI Europe Company) scanning electron microscope the morphology and microstructure of the modified carbon nanofibers were analyzed.

Using ImageJ software, the percentage of SiC nanostructures precipitated on the surface of the tested samples was calculated. The area covered with SiC was marked and its surface was determined. The percentage of the total surface covered with SiC was then determined. For each sample, measurements were repeated on 5 different SEM images and the results were averaged.

The chemical composition of the obtained samples at various stages of thermal treatment was examined using Fourier transform infrared spectroscopy (FTIR Tensor 27, Bruker) in transmittance mode, with a resolution of  $4\text{ cm}^{-1}$ . The standard KBr pellet method was used.

XRD analysis was performed using a Philips X'Pert Pro diffractometer with a Cu K $\alpha$  radiation source ( $\lambda = 0.1542\text{ nm}$ ).

Two bacterial strains were used to assess the microbiological activity of CNFs samples modified with needle-like SiC nanostructures – Gram positive (*S. aureus* ATCC 6538P) and Gram negative (*E. coli* ATCC 8739). The study of the kinetics of bacterial growth in contact with the obtained nanofibrous materials was carried out for 24 h ( $37\text{ }^{\circ}\text{C}/24\text{h}$ ) on a shaker, in a liquid environment and without access to light, following the described procedure (Chen et al., 2012).

Bacterial suspension ( $2\ \mu\text{l}$ ,  $1.2 \times 10^6\text{ CFU}$ ) in 20 ml of culture medium was inoculated onto the prepared material samples with dimensions of 5x5 mm. By measuring the optical density at 600 nm (OD 600) using a UV-Vis spectrophotometer (UV-1800i, Shimadzu), the bacterial growth rate was monitored. The measurement was made at specific time intervals within 24 h. Then the optical density was plotted as a function of the incubation duration.

The number of colonies of Gram positive bacteria (*S. aureus* ATCC 6538P) was determined after 3 h and 24 h, maintaining the conditions described in the procedure (Subhan, 2020).

## 3. Results and Discussion

### 3.1. SEM morphology

Fig. 2 shows the morphology of SiC nanostructures growing on the surface of CNFs. Individual forms of SiC differ in morphology depending on the method of preparing the composite and the SiC precursor used. Figs. 2 a-d show images of CNFs modified volumetrically with SiC precursors, while Figs. 2 e, f) show images of CNFs modified on

the surface. In the case of the CNF/polysiloxane sample (Fig. 2 a, b), thin needles are formed and transform into triangular prisms. This is probably due to the use of temperature too high for the polysiloxane precursor. Silicon carbide needles probably form at temperatures below 1550°C and then transform into prisms. The growth of multi-shaped SiC nanofibers is based on the vapor-solid growth mechanism and changes in the morphology of nanofibers are the result of temperature-dependent growth kinetics (Dai et al., 2017). The use of TEOS as a precursor allowed needle-like structures growing from the surface of carbon nanofibers to be obtained (Fig. 2 c, d). The use of silanization in the  $\frac{T}{D} = \frac{4}{1}$  sol resulted in the growth of nanostructured SiC needles (Figs. 2 e, f). Local transformation of the needles into triangular prisms could also be observed.

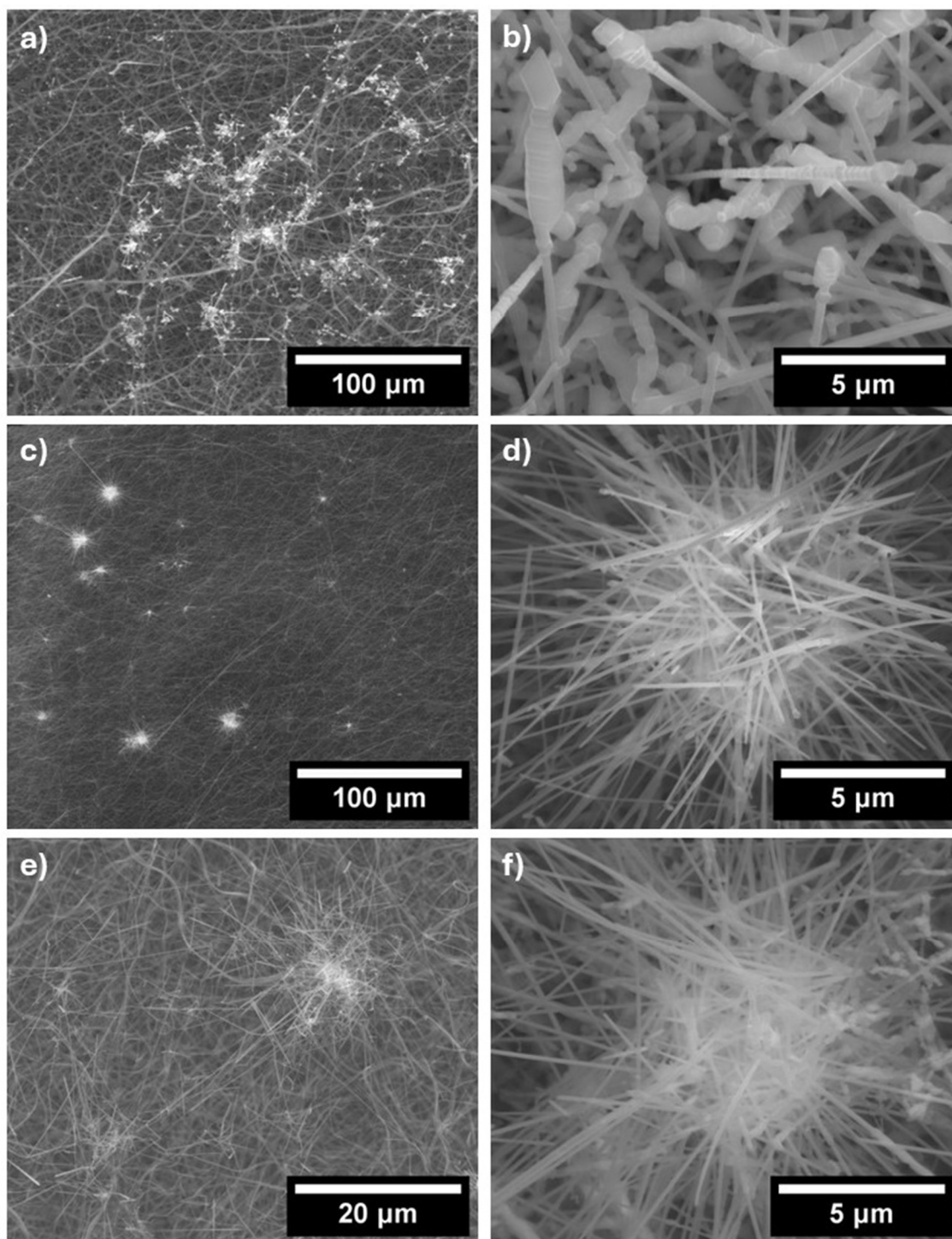


Figure 2. SEM micrographs of a, b) CNF/polysiloxane, c, d) CNF/TEOS, e, f) CNF/sol.

The method of preparing composites and the type of SiC precursor have influence not only on the morphology of SiC nanostructures, but also on the morphology of carbon nanofibers. In the case of CNF/TEOS (Fig. 2 c, d) and CNF/sol (Fig. 2 e, f) samples, the carbon nanofibers are uniform along their entire length. They create a system of entangled nanofibers. The use of polysiloxane as a SiC precursor had the strongest

impact on fiber morphology. The nanofibers took the form of branched structures, stuck together in places. The presence of polysiloxane in an amount of 50% of the mass of PAN causes changes in the viscosity of the spinning solution and probably slows down the solvent evaporation process, causing the obtained nanofibers to be more flattened, stuck together, and thus having a larger diameter (Figs. 3 c, d and 4) (Manea et al., 2015).

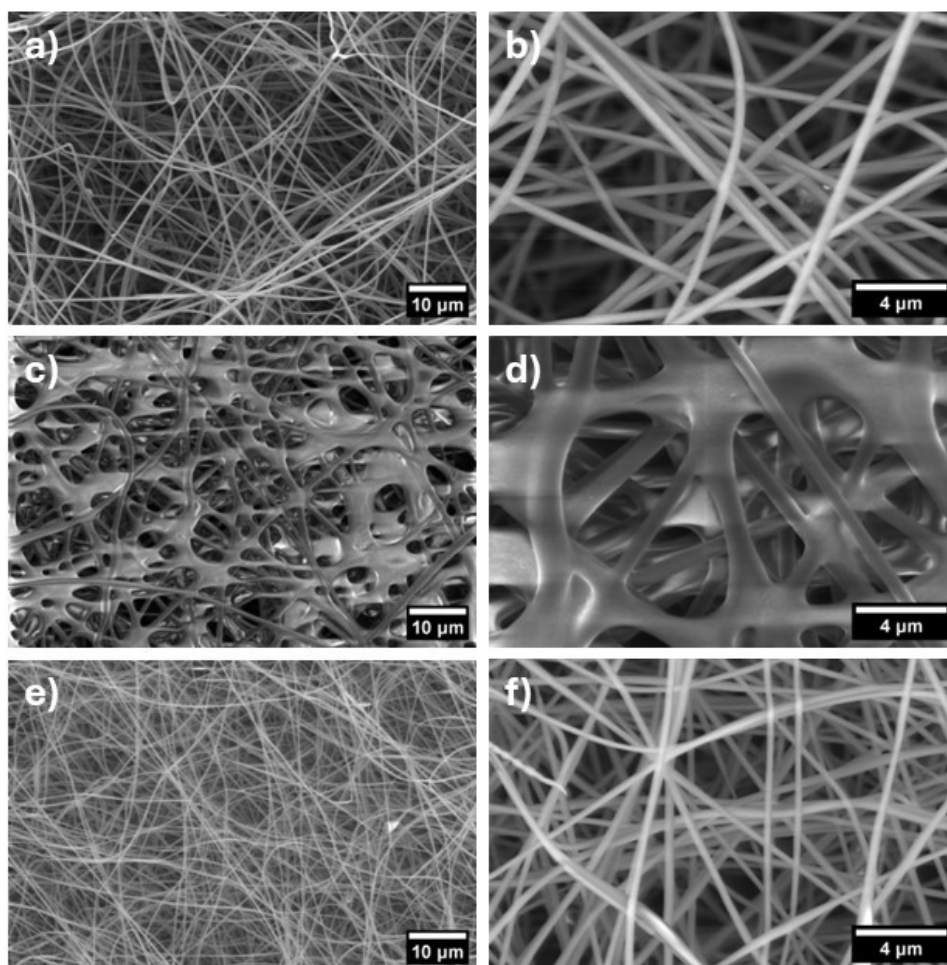


Figure 3. SEM micrographs of a, b) PAN nanofibers, c, d) PAN/polysiloxane, and e, f) CNF/TEOS.



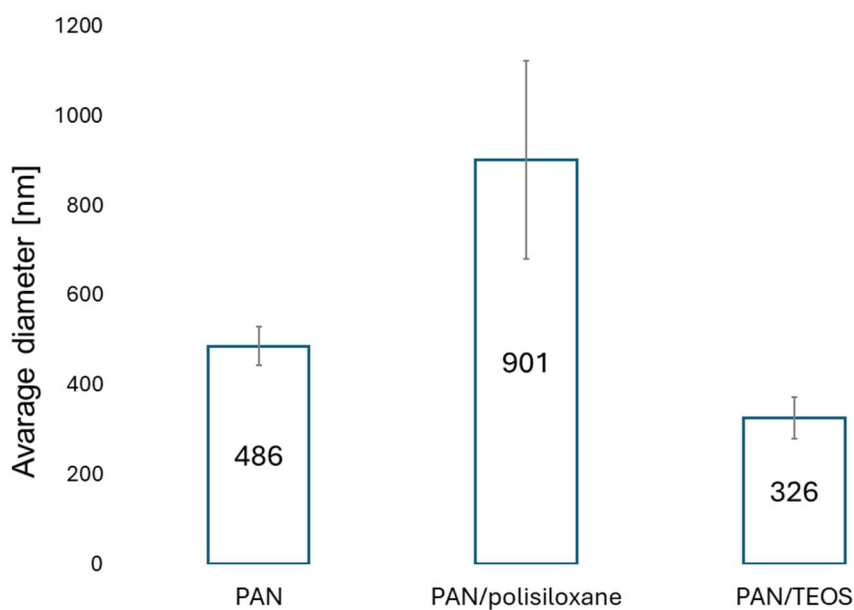


Figure 4. Average diameter of PAN nanofibers before and after modification.

Significant differences were also observed in the diameters of carbon nanofibers (Fig. 5). The diameters of carbon nanofibers have different values depending on the SiC precursor used. The highest diameter values of carbon nanofibers were observed for materials volumetrically modified with polysiloxane, while the lowest values of diameters were observed in the case of the CNF/TEOS sample. A significant change in the diameters of CNF/polysiloxane nanofibers compared to CNF nanofibers without modification (increase by 145%) was observed already at the stage of obtaining polymer precursors (Fig. 4). The highest standard deviation value was also recorded for this sample, which shows that the obtained nanofibers were non-uniform in terms of diameters. Probably, the addition of TEOS to a 10% PAN solution reduces the viscosity, and thus the formed PAN/TEOS nanofibers are smaller (Fig. 4). This also has a direct impact on the lower diameter of the nanofiber after carbonation (Fig. 5). Modification of the CNF surface because of silanization in a sol containing T and D structural units in molar proportions  $T/D = 4/1$  resulted in an increase of approximately 13% compared to CNF fibers without modification. This may suggest that an additional layer is formed on the CNF surface as a result of thermal treatment of the sol.

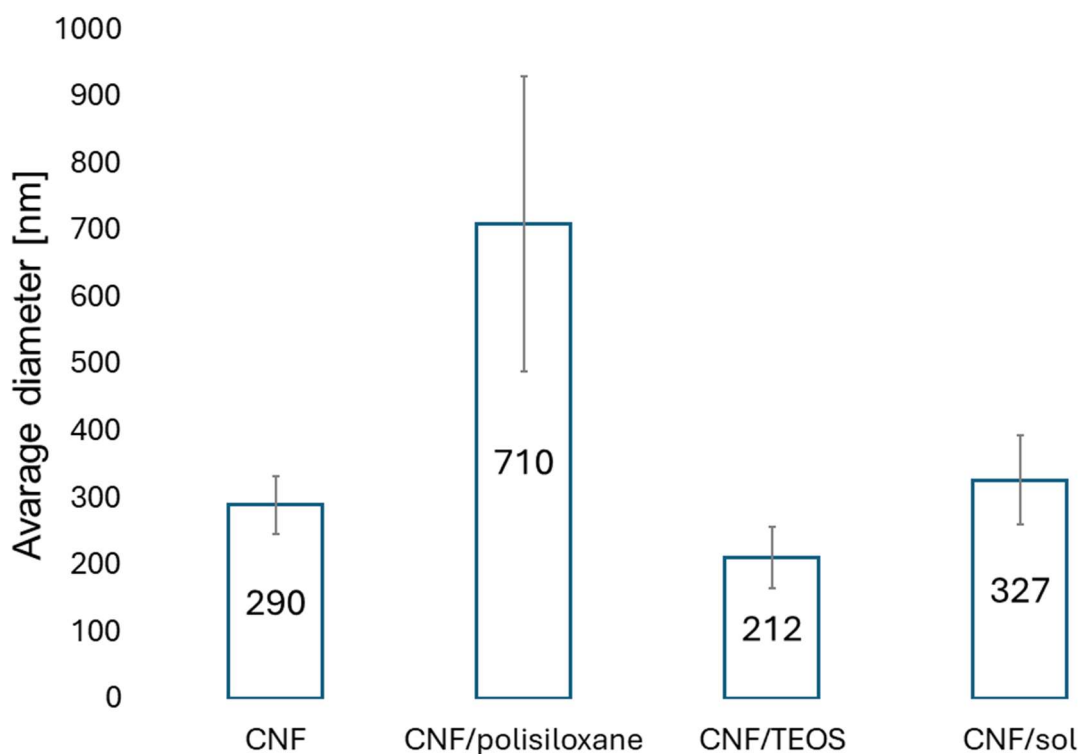


Figure 5. Average diameter of CNF nanofibers before and after modification.

Moreover, the type of precursor used, and the method of modification influenced differences in the number of SiC nanostructures formed on the surface of the samples. Based on SEM images, the percentage of surface areas of samples covered with SiC nanostructures was estimated: CNF/polysiloxane 35%, CNF/TEOS 5%, CNF/sol 25%.

### 3.2. FT-IR analysis

Analyzing the FT-IR spectra of the tested materials (Fig. 6), the presence of Si-C bands at  $740\text{--}780\text{ cm}^{-1}$ , originating from stretching vibrations, was observed in each of the tested samples, and they differed in intensity (Kaneko et al., 2005). For volume-modified samples (Fig. 6 a, b), the Si-C group is visible after carbonization at a temperature of  $1550\text{ }^{\circ}\text{C}$ , while for surface-modified systems (Fig. 6 c) this band is observed after thermal treatment at  $800\text{ }^{\circ}\text{C}$ . This suggests that the use of silanization in sol favors the formation of SiC structures at lower temperatures. Each of the presented spectra shows the presence of bands at approximately  $1050\text{--}1100\text{ cm}^{-1}$  originating from asymmetric stretching vibrations of Si-O-Si bonds (Kim et al., 2010). Moreover, Figs. 6 a and b show the spectra of polymer nanofibers before thermal treatment. They contain bands

characteristic of polyacrylonitrile, which disappear as stabilisation progresses (Karbownik et al., 2015).

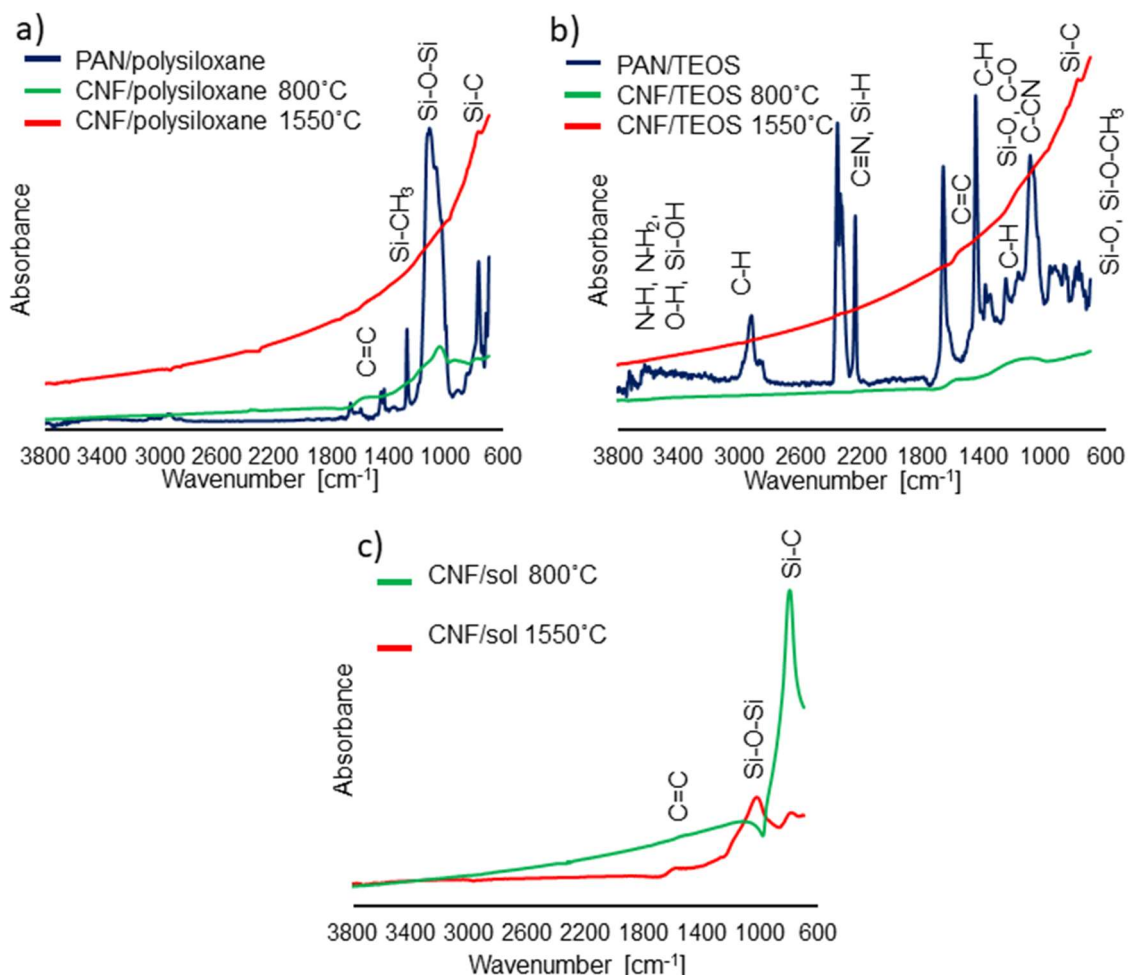


Figure 6. FTIR spectra of a) CNF/polysiloxane, b) CNF/TEOS, c) CNF/sol.

### 3.3. XRD analysis

The XRD analysis shown in Fig. 7 confirms the presence of SiC in CNF/polysiloxane and CNF/sol. Diffraction peaks correspond to the cubic polytype  $\beta$ -SiC. Moreover, in the tested systems there are diffraction peaks between  $20^\circ$  and  $30^\circ$  coming from the amorphous carbon phase (Nhut et al., 2004). The absence of the SiC phase observed in the diffractogram Fig 7 b) is probably related to the collection of a sample fragment for XRD analysis. Analyzing SEM photos of the tested materials, it was observed that the needle-like SiC nanostructures were not evenly distributed throughout the sample volume (Fig. 2 d).

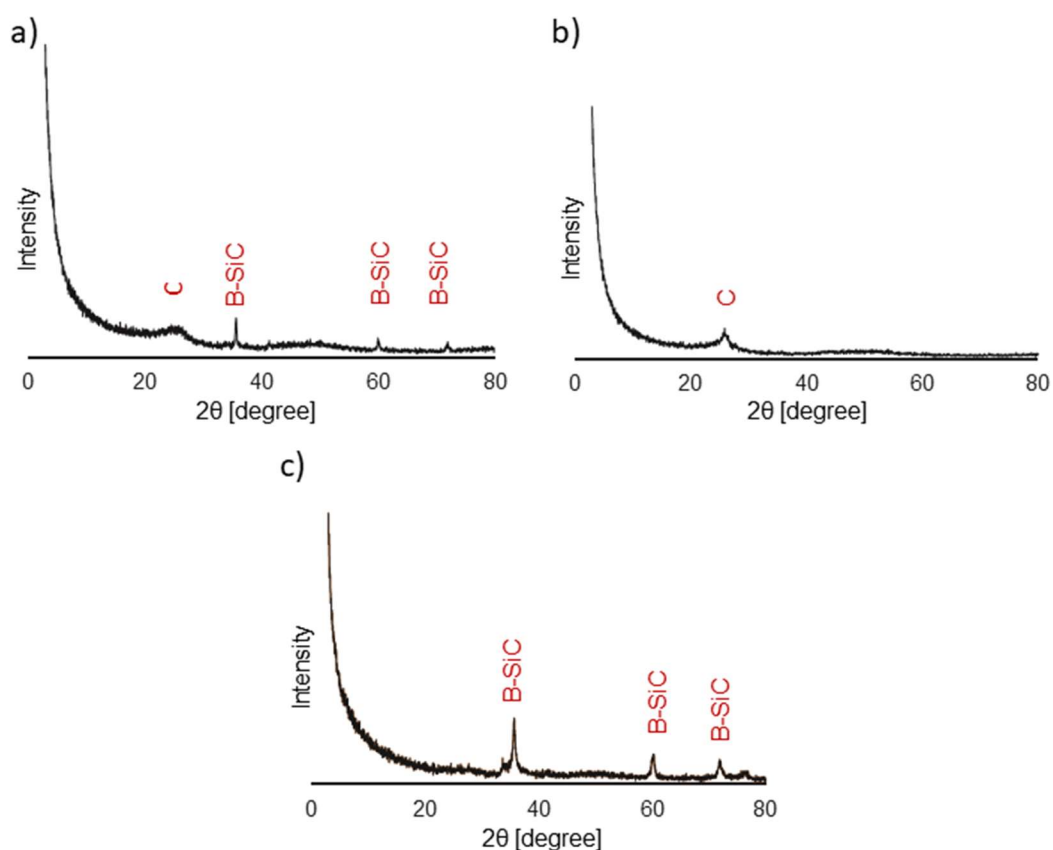


Figure 7. XRD analysis of a) CNF/polysiloxane, b) CNF/TEOS, c) CNF/sol.

### 3.4. Microbiology test

Analyzing the bacterial growth curves (Figs. 8 a, b), a clear increase in the number of both strains was observed in contact with CNFs constituting a reference sample. An increase in the number of bacteria, depending on the method of modification used, is also visible for modified samples. CNFs modified with organosilicon compounds do not affect Gram-negative bacteria (*Escherichia coli*), but they show some microbiological activity in contact with Gram-positive bacteria (*Staphylococcus aureus*). The inhibition of the growth of *Staphylococcus aureus* multiplication is especially visible for the CNF/sol and CNF/polysiloxane samples. These samples are characterised by some bacteriostatic properties. Unlike Gram-positive bacteria, Gram-negative bacteria have an additional lipopolysaccharide (LPS) layer in their structure that provides protection against external factors, which makes them less sensitive to the bacteriostatic effect (Maldonado et al., 2016). The bacteriostatic effect was probably caused by the presence of needle-like SiC nanostructures in the tested materials. The influence of structural morphology of different materials including nanomaterials on the microbial response is widely described in the literature (Babayevska et al., 2022; Gandotra et al., 2021;

Stanković et al., 2013; Szala and Borkowski, 2014). The shape of the obtained SiC nanostructures may be a decisive factor. The inhibition of bacterial growth and multiplication was probably due to mechanical damage to the integrity of the bacterial cell membrane by SiC nanostructures. Disruption of the integrity of the bacterial cell membrane causes oxidative stress leading to growth inhibition, cytotoxicity, and even death of the bacteria (Selim et al., 2020). The antibacterial effect is probably based on the synergy of mechanical damage to the bacterial cell and the production of reactive oxygen species (Gandotra et al., 2021). The toxic effect of SiC nanofibers and nanorods obtained by combustion synthesis on bacteria is known from the literature (Szala and Borkowski, 2014). To date, the antibacterial activity of needle-like SiC nanostructures as modifiers of CNFs has not been investigated.

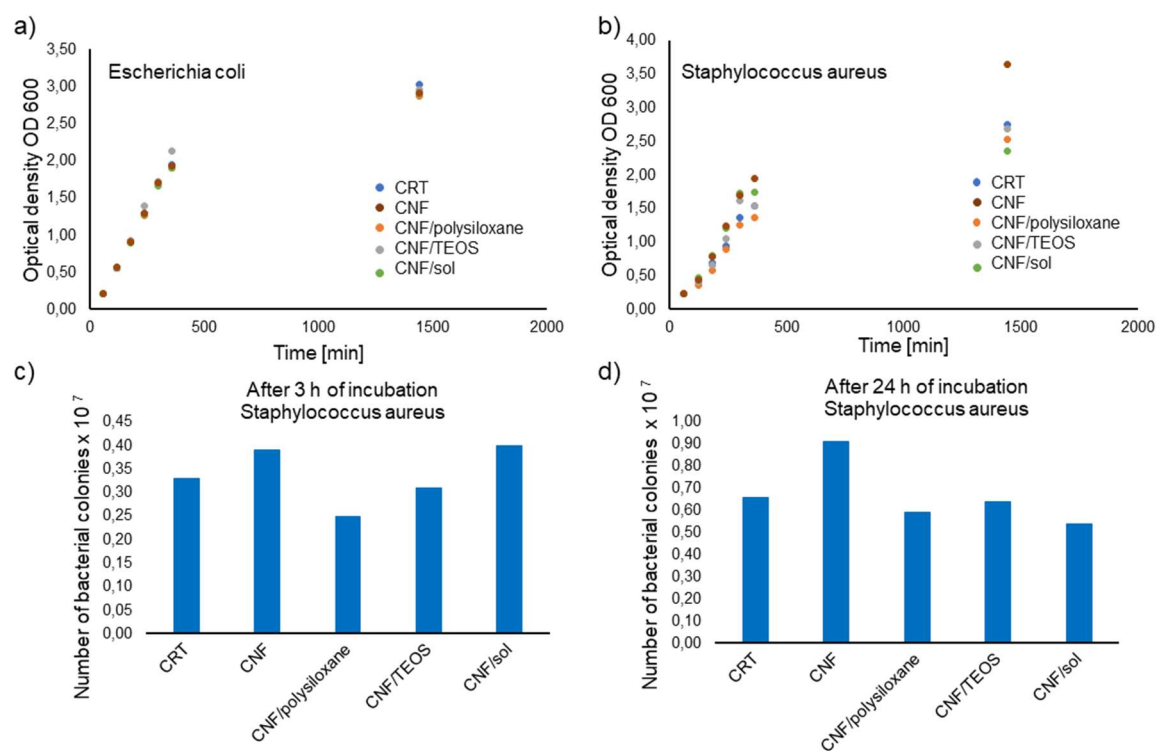


Figure 8. Growth curves of bacterial grown from the tested materials in the culture media system a) *Escherichia coli*, b) *Staphylococcus aureus* and the number of *Staphylococcus aureus* colonies in contact with the tested materials after c) 3 h and d) 24 h of incubation.

#### 4. Conclusions

The aim of the work was to obtain hierarchical ceramic-carbon systems in which needle-like SiC nanostructures grow on the surface of CNFs. Three types of modifications were carried out using three different SiC precursors. The obtained nanocomposite systems were assessed in terms of morphology and microstructure. SEM observations showed the presence of needle-like nanostructures on the surface of the CNFs, but the number

of precipitates varied depending on the modifier used. The use of polysiloxane as a SiC precursor resulted in the greatest amount of needle-like structures. FT-IR analysis confirmed the presence of Si-C groups in all tested systems, while XRD allowed the identification of the SiC phase as the  $\beta$ -SiC polytype in CNF/polysiloxane and CNF/sol systems. Microbiological tests showed CNF/sol and CNF/polysiloxane bacteriostatic properties, suggesting their potential for filter materials inhibiting bacterial growth. This effect likely stems from the toxic impact of needle-like SiC nanostructures on bacterial cells.

### Acknowledgments

This research project was supported by the program “Excellence initiative—research university” from the AGH University of Krakow, project no. 1580.

### References

- Babayevska N., Przysiecka Ł., Iatsunskiy I., Nowaczyk G., Jarek M., Janiszewska E., Jurga S., 2022. ZnO size and shape effect on antibacterial activity and cytotoxicity profile. *Sci. Rep.*, 12(1), 1–13. DOI: 10.1038/s41598-022-12134-3.
- Chen S., Guo Y., Chen S., Yu H., Ge Z., Zhang X., Zhang P., Tang J., 2012. Facile preparation and synergistic antibacterial effect of three-component Cu/TiO<sub>2</sub>/CS nanoparticles. *J. Mater. Chem.*, 22(18), 9092–9099. DOI: 10.1039/c2jm00063f.
- Cheng C., Li X., Yu X., Wang M., Wang X., 2018. Electrospun nanofibers for water treatment, In: *Electrospinning: Nanofabrication and Applications*. Elsevier Inc., 419-453. DOI: 10.1016/B978-0-323-51270-1.00014-5.
- Dai J., Sha J., Zhang Z., Shao J., Zu Y., Lei M., 2017. Catalyst-free growth of multi-shaped SiC nanofibers on carbon fibers at elevated temperatures. *Ceram. Int.*, 43(18), 17057–17063. DOI: 10.1016/j.ceramint.2017.09.119.
- Faccini M., Borja G., Boerrigter M., Morillo Martín D., Martínez Crespiera S., Vázquez-Campos S., Aubouy L., Amantia D., 2015. Electrospun Carbon Nanofiber Membranes for Filtration of Nanoparticles from Water. *J. Nanomater.*, 2015. DOI: 10.1155/2015/24747.
- Gandotra R., Chen Y. R., Murugesan T., Chang T. W., Chang H. Y., Lin H. N., 2021. Highly efficient and morphology dependent antibacterial activities of photocatalytic Cu<sub>x</sub>O/ZnO nanocomposites. *J. Alloys Compd.*, 873, 159769. DOI: 10.1016/j.jallcom.2021.159769.
- Kaneko T., Nemoto D., Horiguchi A., Miyakawa N., 2005. FTIR analysis of a-SiC:H films grown by plasma enhanced CVD. *J. Cryst. Growth*, 275(1–2), 1097–1101.

- DOI: 10.1016/j.jcrysgr.2004.11.128.
- Karbownik I., Fiedot M., Rac O., Suchorska-Woźniak P., Rybicki T., Teterycz H., 2015. Effect of doping polyacrylonitrile fibers on their structural and mechanical properties. *Polymer*, 75(August), 97–108. DOI: 10.1016/j.polymer.2015.08.015.
- Kim B. H., Kim C. H., Yang K. S., Kim K. Y., Lee Y. J., 2010. SiC/SiO<sub>2</sub> coating for improving the oxidation resistive property of carbon nanofiber. *Appl. Surf. Sci.*, 257(5), 1607–1611. DOI: 10.1016/j.apsusc.2010.08.104.
- Koyanagi T., Terrani K., Harrison S., Liu J., Katoh Y., 2021. Additive manufacturing of silicon carbide for nuclear applications. *J. Nucl. Mater.*, 543, 152577. DOI: 10.1016/j.jnucmat.2020.152577.
- Maldonado R. F., Sá-Correia I., Valvano M. A., 2016. Lipopolysaccharide modification in gram-negative bacteria during chronic infection. *FEMS Microbiol. Rev.*, 40(4), 480–493. DOI: 10.1093/femsre/fuw007.
- Manea L. R., Scarlet R., Amariei N., Nechita E., Sandu I. G., 2015. Study on behaviour of polymer solutions in electrospinning technology. *Revista de Chimie*, 66(4), 542–546.
- Nhut J. M., Pesant L., Keller N., Pham-Huu C., Ledoux M. J., 2004. Pd/SiC exhaust gas catalyst for heavy-duty engines: Improvement of catalytic performances by controlling the location of the active phase on the support. *Top. Catal.*, 30–31(July), 353–358. DOI: 10.1023/b:toca.0000029774.03973.a6.
- Pazdyk-Slaby W., Stodolak-Zych E., Zambrzycki M., Zych L., Gubernat M., Swietek M., Smolka W., Fraczek-Szczypta A., 2024. Preparation of electrospun carbon nanofibers (eCNF) modified with metal compounds with antibacterial properties. *J. Environ. Chem. Eng.*, 12(4), 113185. DOI:10.1016/j.jece.2024.113185.
- Selim M. S., Mo P. J., Hao Z., Fathallah N. A., Chen X., 2020. Blade-like structure of graphene oxide sheets decorated with cuprous oxide and silicon carbide nanocomposites as bactericidal materials. *J. Colloid Interface Sci.*, 578, 698–709. DOI: 10.1016/j.jcis.2020.06.058.
- Sharon M., 2021. An Introduction to Carbon Nanofiber. In: *Carbon Nanofibers: Fundamentals and Applications*, 2, 1–20. DOI: 10.1002/9781119769149.ch1.
- Soltani S., Khanian N., Roodbar Shojaei T., Shean Yaw Choong T., Asim, N. 2022. Fundamental and recent progress on the strengthening strategies for fabrication of polyacrylonitrile (PAN)-derived electrospun CNFs: Precursors, spinning and collection, and post-treatments. *J. Ind. Eng. Chem.*, 110, 329–344. DOI: 10.1016/j.jiec.2022.03.005.
- Stanković A., Dimitrijević S., Uskoković D., 2013. Influence of size scale and

- morphology on antibacterial properties of ZnO powders hydrothermally synthesized using different surface stabilizing agents. *Colloids Surf., B.*, *102*, 21–28. DOI: 10.1016/j.colsurfb.2012.07.033.
- Subhan M. A., 2020. Antibacterial property of metal oxide-based nanomaterials. In *Nanotoxicity: Prevention and Antibacterial Applications of Nanomaterials*. INC. 283-300. DOI: 10.1016/B978-0-12-819943-5.00013-0.
- Szala M., Borkowski A., 2014. Toxicity assessment of SiC nanofibers and nanorods against bacteria. *Ecotoxicol. Environ. Saf.*, *100*(1), 287–293. DOI: 10.1016/j.ecoenv.2013.10.030.
- Tan J., Zhang J., Zhong H., Hu H., Kou X., Zhang B., 2024. Organosilicon-grafted silica nanoparticles for vat photopolymerization: Evolution from organic/inorganic hybrid materials to ceramics. *Open Ceram.*, *17*(October 2023), 100513. DOI: 10.1016/j.oceram.2023.100513.
- Xu G., Yamakami T., Yamaguchi T., Endo M., Taruta S., Kubo I., 2014. Surface modification of carbon nanofibers with SiC by heating different SiO vapor sources in argon atmosphere. *J. Ceram. Soc. Jpn.*, *122*(1429), 822–828. DOI: 10.2109/jcersj2.122.822.
- Zhao R., Wang Y., Li X., Sun B., Li Y., Ji H., Qiu J., Wang C., 2016. Surface Activated Hydrothermal Carbon-Coated Electrospun PAN Fiber Membrane with Enhanced Adsorption Properties for Herbicide. *ACS Sustainable Chem. Eng.*, *4*(5), 2584–2592. DOI: 10.1021/acssuschemeng.6b00026.